

See discussions, stats, and author profiles for this publication at: <https://www.researchgate.net/publication/256439817>

Thermochromism in Polydiacetylene-ZnO Nanocomposites

ARTICLE *in* THE JOURNAL OF PHYSICAL CHEMISTRY C · SEPTEMBER 2013

Impact Factor: 4.77 · DOI: 10.1021/jp403939p

CITATIONS

8

READS

39

5 AUTHORS, INCLUDING:



Aide Wu

Tulane University

8 PUBLICATIONS 22 CITATIONS

[SEE PROFILE](#)



Christian Beck

New Jersey Institute of Technology

2 PUBLICATIONS 14 CITATIONS

[SEE PROFILE](#)



Zafar Iqbal

New Jersey Institute of Technology

247 PUBLICATIONS 6,173 CITATIONS

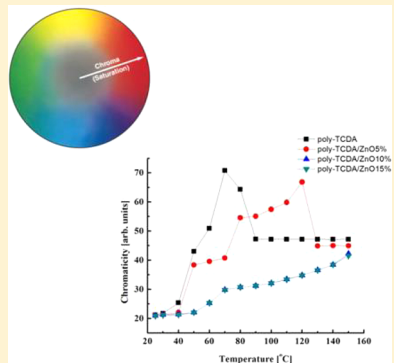
[SEE PROFILE](#)

Thermochromism in Polydiacetylene–ZnO Nanocomposites

Aide Wu,[†] Christian Beck,[‡] Ye Ying,[‡] John Federici,[†] and Zafar Iqbal*,[‡]

[†]Department of Physics, and [‡]Department of Chemistry and Environmental Science, New Jersey Institute of Technology, Newark, New Jersey 07102, United States

ABSTRACT: Room temperature attenuated total reflection (ATR)-Fourier transform infrared (FTIR), temperature-dependent Raman, colorimetric (using optical densitometry), and differential scanning calorimetry (DSC) are used to provide a qualitative mechanism of the thermochromic reversibility introduced by composite formation of poly-10,12-tricosadiynoic acid (poly-TCDA) with ZnO in the particle size range below 100 nm. The results indicate that in pure poly-TCDA, heating above the chromatic blue to red transition temperature leads to an irreversible stress on the polymer backbone due to break up of hydrogen bonding on the side chain head groups to form an irreversible red phase. By contrast, poly-TCDA composites with nanosize ZnO at concentrations above 5 wt % display rapid chromatic reversibility. Reversibility is only partial for composites with 5 wt % ZnO, and interestingly for composites only of this composition the Raman data indicate a broad scattering band which can be assigned to the irreversible formation of an amorphous poly-TCDA/5 wt % ZnO phase network. The appearance of a new line at 1540 cm^{-1} in the ATR-FTIR spectra of poly-TCDA/ZnO composites is indicative of chelation between head groups on neighboring side chains and ZnO, which facilitates the release of stress on cooling from the red phase to rapidly form the blue phase. Moreover, the colorimetric data show an increase in chromatic transition temperature with increase of the amount of ZnO from 5 to 15 wt % in poly-TCDA. The potential of these nanocomposites as thermochromic temperature sensors is also considered.



1. INTRODUCTION

Chromatic sensors play an important role in different types of sensing. The main advantage of a chromatic sensor is that it provides visual color indication without the need to convert to a digital signal.¹ Polydiacetylenes (PDAs), have been widely studied as a chromatic sensor material because they can respond to mechanical, temperature, and chemical stimuli.^{2–6} Solid state topotactic photopolymerization of diacetylene monomers by exposure to UV or γ -radiation and subsequent thermochromism in closely packed and uniformly ordered thin films of various PDAs are well-known⁷ and have been widely studied for temperature-sensing applications.

PDAs have a one-dimensional conjugated backbone with a strong π to π^* absorption band in the red spectral region of the optical spectrum which gives rise to an intense blue color in the polymer. The blue phase undergoes a heat-induced thermochromic transition observed in many PDAs to a red phase. The blue to red chromatic transition is either irreversible or reversible under heating and cooling cycles depending on the chemical structure and interactions on the side chains of the PDA. In the blue phase, the strain induced by hydrogen bonding at the head groups leads to an increase in π -electron conjugation length. However, when hydrogen bonding interactions are disrupted by heat, the side group strain is released leading to twisting of the π -electron orbitals, decrease of π -electron conjugation,⁸ and concomitant transition to a red phase. The red phase can rapidly reverse back to the blue phase on cooling when interactions due to (a) strong head aromatic groups,⁹ (b) ionic moieties,¹⁰ and (c) covalent bond,^{11,12}

enhanced hydrogen,^{13–18} and multibonding bonding at the head groups^{19–21} are present in the PDA structures. The red phase is irreversible when the head group interactions cannot be restored on cooling. These PDAs are therefore either irreversible or reversible sensors.

PDAs prepared from 10,12-pentacosadiynoic acid (PCDA) and 10,12-docosadiynedioic acid (DCDA) have been widely investigated,^{22–24} but little attention has been given to the related but important monomer with a shorter hydrocarbon side chain, $\text{CH}_3(\text{CH}_2)_9-\text{C}\equiv\text{C}-\text{C}\equiv\text{C}-(\text{CH}_2)_7\text{CH}_2\text{COOH}$ (10,12-tricosadiynoic acid, TCDA). Previous work performed in this group (Patlolla et al.²⁵) on poly-PCDA–metal oxide nanocomposites provided a broad understanding of the changes in chromatic properties of the nanocomposites relative to those of pure PCDA. Here a more detailed investigation is carried out using Raman spectroscopy, DSC, and colorimetry using optical densitometry as a function of temperature on poly-TCDA and poly-TCDA/ZnO nanocomposites, together with an ATR-FTIR study at ambient temperature to extract a molecular level understanding of poly-TCDA/ZnO nanocomposite formation.

2. EXPERIMENTAL SECTION

2.1. Materials. TCDA was purchased from GFS Chemicals, and nanocrystalline ZnO (<100 nm diameter) was purchased

Received: April 21, 2013

Revised: August 29, 2013

Published: September 3, 2013



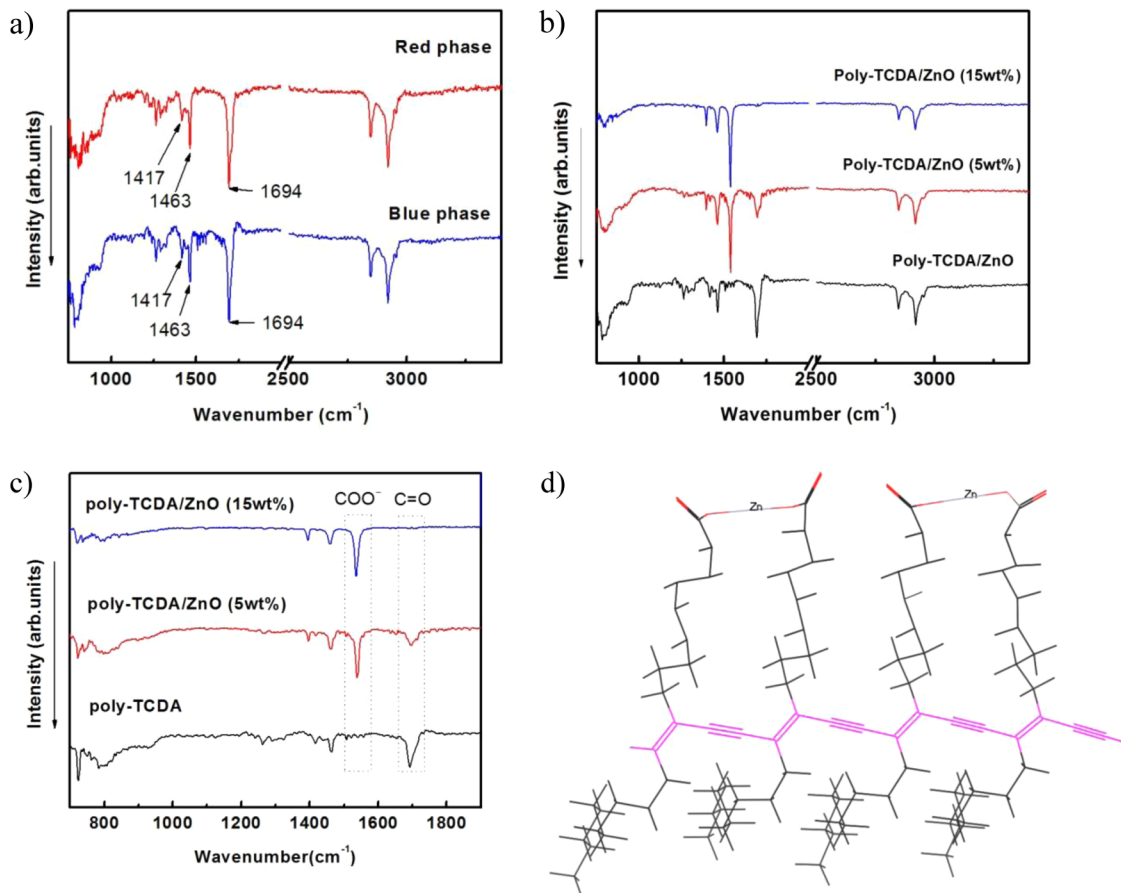


Figure 1. ATR-FTIR spectra at room temperature of (a) pure poly-TCDA in the blue and red phases and (b) and (c) poly-TCDA and poly-TCDA/ZnO in the blue phase for two concentrations of ZnO between 700 and 3300 cm⁻¹ and expanded in the 750 and 1800 cm⁻¹ spectral range, respectively. Panel (d) shows a computer-generated approximate model of the chelate proposed.

from Sigma-Aldrich. Analytical grade chloroform was purchased from Sigma-Aldrich and used without further purification.

2.2. Synthesis of Poly-TCDA-ZnO Nanocomposites.

Poly-TCDA/ZnO suspensions were prepared by suspending different amounts of ZnO (5, 10, 15 wt %) in solution of the TCDA monomer (1 mM) in chloroform. The suspension contained in a beaker was sonicated in a water bath at room temperature for 30 min and dried at 40 °C with magnetic stirring for 8 h. The magnetic stirring was stopped after the liposome state was achieved. The pure TCDA and TCDA composites were polymerized to the blue phase of poly-TCDA and poly-TCDA-ZnO composite by irradiating with a 254 nm wavelength UV source. Powders of the blue phase composite were obtained by scraping from the beaker and grinding into a fine powder. Red phase composite powders and films were similarly produced after heating the blue phase to above the thermochromic transition temperature.

2.3. Raman Spectroscopy.

Raman spectra at room temperature were obtained primarily using a Mesophotonics Raman spectrometer with 785 nm laser excitation. Temperature-dependent Raman measurements were carried out with an EZRaman LE Raman Analyzer system from Optronics using 785 nm laser excitation coupled to a Leica optical microscope. The spectrometer was calibrated using silicon wafer and diamond powder standards to a frequency accuracy of 1 cm⁻¹. The variable temperature optical stage used is from Linkam Scientific Instruments Ltd. Thick films for the Raman measurements were prepared by mixing suspensions of TCDA

with a certain amount of ZnO, using chloroform as the suspension medium. After drying and 254 nm UV radiation, the polymerized dry powders of poly-TCDA and poly-TCDA/ZnO were measured on a silicon wafer substrate.

2.4. ATR-FTIR Spectroscopy. Fourier transform infrared (FTIR) was carried out using a Nicolet ThermoElectron FTIR 560 spectrometer with a MIRacle attenuated total reflectance (ATR) platform assembly and a Ge plate.

2.5. Optical Densitometry. Chromaticity, which is a quantitative measure of the vividness or dullness of a color (or how close the color is to either the gray or pure hue), was measured directly on thin film and coated samples using an X-Rite 518 optical densitometer as the samples were heated on a temperature-controlled hot plate.

2.6. Differential Scanning Calorimetry (DSC). A Mettler Toledo DSC instrument (Mettler-Toledo Inc., Columbus, OH) with a FP90 central processor was used to obtain the DSC data of 10 mg of precursor, polymer, and composite samples wrapped in a small disk with aluminum foil using heating/cooling/heating cycles in the temperature range from 25 to 300 °C at a rate of 10 °C min⁻¹.

3. RESULTS AND DISCUSSION

Attenuated total reflection (ATR)-Fourier transform infrared (FTIR) spectroscopy at room temperature in both the red and blue phases for pure poly-TCDA and for the blue phase in poly-TCDA/ZnO together with Raman spectroscopy as a function of temperature for poly-TCDA and poly-TCDA/ZnO

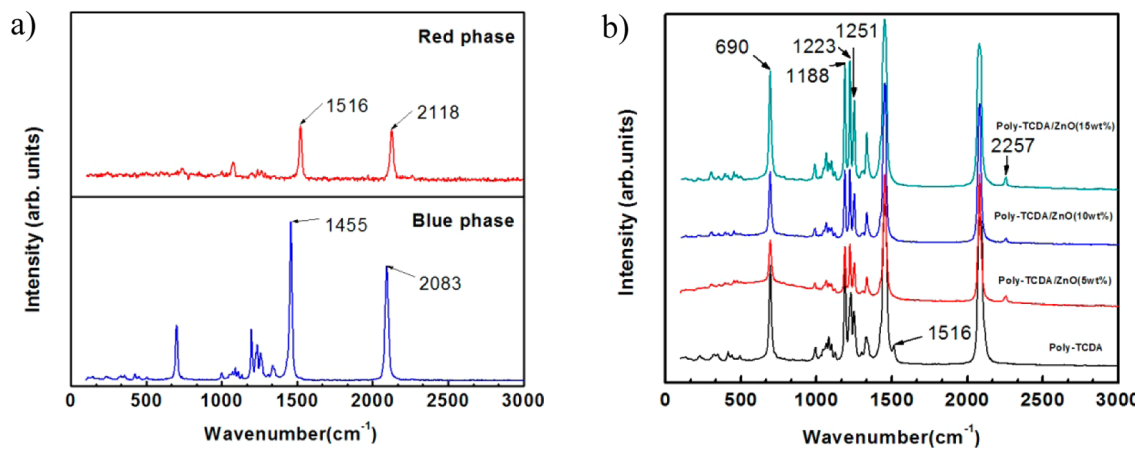


Figure 2. Laser-excited (785 nm) Raman spectra of (a) blue (bottom) and red (top) phases of poly-TCDA at room temperature; (b) blue phase of poly-TCDA and poly-TCDA/ZnO composites with three different ZnO concentrations at ambient temperature.

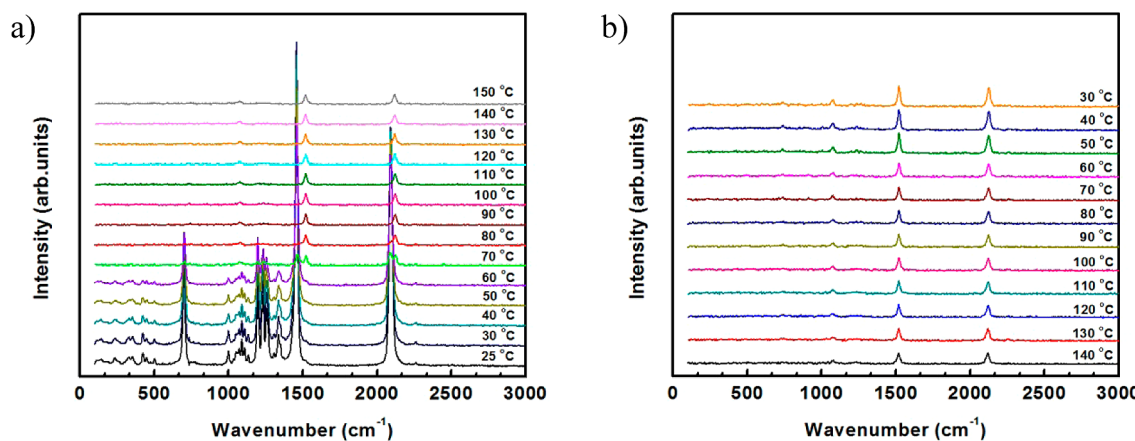


Figure 3. Laser excited (785 nm) Raman spectra of pure poly-TCDA as a function of (a) increasing temperature and (b) decreasing temperature.

provides details about the molecular structural changes around the chromatic transition and molecular interactions on nanocomposite formation. The thermal and colorimetric changes as a function of temperature at these transitions are investigated further by DSC and optical densitometry, respectively.

Figure 1a shows the ATR-FTIR spectra of poly-TCDA in its blue and red phases, and Figures 1b and 1c show the spectra of poly-TCDA and poly-TCDA/ZnO in the 700–3500 cm⁻¹ and expanded in the 700–1900 cm⁻¹ regions, respectively. Lines at 2920 and 2847 cm⁻¹ are assigned to the asymmetric and symmetric stretching vibrations, respectively, of the CH₂ groups on the side chains, and those at 1463, 1417, and 1694 cm⁻¹ can be attributed to the CH₂ scissoring and hydrogen-bonded carbonyl C=O stretching vibrations, respectively. On comparing the FTIR spectra of pure poly-TCDA with that of poly-TCDA/ZnO shown in Figures 1b and 1c, it is observed that a relatively strong new line appears at 1540 cm⁻¹ in the spectrum of poly-TCDA/ZnO together with a concomitant decrease in intensity of the C=O stretching line at 1694 cm⁻¹. The 1540 cm⁻¹ line can be assigned to an asymmetric COO⁻ stretching vibration, and its presence in the spectra together with a corresponding decrease in the intensity of the C=O line suggests that a chelate between neighboring side chain -COOH head groups of poly-TCDA and Zn²⁺ ions from ZnO is formed (see computer-generated approximate model in

Figure 1d). This chemical interaction between ZnO and poly-TCDA, dependent on the ionicity of the Zn–O bond, is likely to cause the high temperature red phase to reverse back to the blue phase on cooling²⁶ in poly-TCDA/ZnO composites.

Raman scattering due to the molecular vibrational modes of the conjugated polymer backbone is expected to be primarily resonance-enhanced for excitation using 780 nm laser radiation. From the Raman spectra in Figure 2a for pure poly-TCDA, two intense lines at 2083 and 1455 cm⁻¹ are observed at room temperature in the blue phase, which can be definitively assigned to the C≡C and C=C stretching modes of the polymer backbone, respectively. Note that the C=C stretching mode is close in frequency to a line at 1463 cm⁻¹ assigned to a side chain CH₂ deformation mode observed in the ATR-FTIR spectra in Figure 1. In the red phase the room temperature C≡C and C=C stretching vibration frequencies at 2114 and 1516 cm⁻¹, respectively, increase due to the irreversible stress on the polymer backbone. The line intensities in the red phase are lower because of decreased resonance interaction with the polymer backbone. This decrease in resonance interaction with the polymer backbone in the red phase was not evident in the Raman spectrum of the red phase of PCDA²⁵ and is likely to be due to the fact that the hydrocarbon side chain is longer in PCDA. The Raman lines at frequencies below that of the C=C stretching mode can be assigned to Raman-

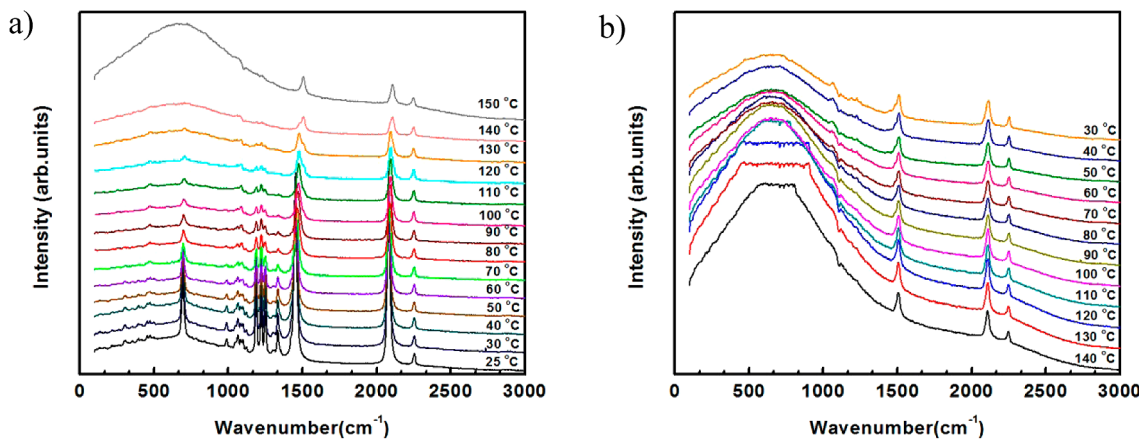


Figure 4. Laser-excited (785 nm) Raman spectra of poly-TCDA/ZnO (5 wt %) as a function of (a) increasing temperature and (b) decreasing temperature.

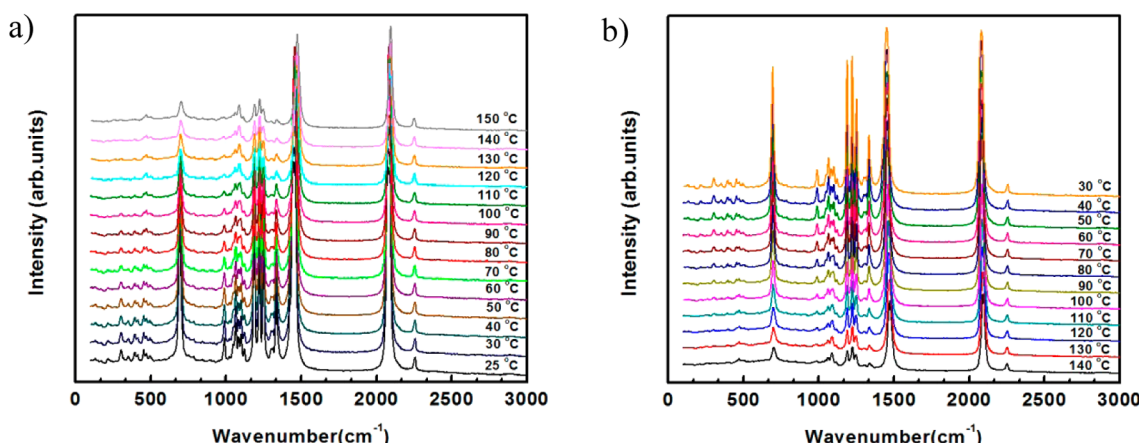


Figure 5. Laser-excited (785 nm) Raman spectra of poly-TCDA/ZnO (15 wt %) as a function of (a) increasing temperature and (b) decreasing temperature.

active deformation and C–C stretching motions of the conjugated polymer backbone mixed with hydrocarbon chain deformation modes. The triplet of lines around 1250 cm⁻¹ and the line at 690 cm⁻¹ in the blue phase are relatively intense as a result of resonance enhancement due to mixing of the backbone C–C stretching and deformation modes.

Figure 2b shows the Raman spectrum of pure poly-TCDA in the blue phase compared with the blue phase spectra of poly-TCDA/ZnO composites. From Figure 2b, it is evident that a very weak line at 2257 cm⁻¹ in the C≡C stretching mode region of poly-TCDA increases in intensity in the composite. By contrast a relatively weak line in the C=C region at 1516 cm⁻¹ in the blue phase due to a red phase impurity disappears on composite formation. The line at 2257 cm⁻¹ can be assigned to a diyne defect formed on the backbone due to the chemical interaction between TCDA and ZnO.²⁶ However, the intensity of this line appears to saturate at low ZnO concentration and does not increase with increasing ZnO. Another interesting feature in Figure 2b which is consistent with the chemical interaction of poly-TCDA with ZnO is that the line at 690 cm⁻¹ and the triplet of lines at 1250 cm⁻¹ assigned above to largely polymer backbone modes show substantial increase in intensity in the composite phase.

Raman spectra under heating and cooling cycles in the 25–150 °C temperature range for poly-TCDA and poly-TCDA/ZnO at different ZnO concentrations are shown in Figures

3–5. The Raman data were taken in steps of 10 °C from 30 to 150 °C and also recorded in 10 °C steps during the cool down to room temperature. Figure 3 displays the Raman spectra of poly-TCDA with increasing temperature to 150 °C followed by cooling from 140 to 30 °C. From the heat-up spectra in Figure 3a, it can be observed that the backbone stretching and deformation lines in the blue phase decrease in intensity with increasing temperature as the sample goes to the red phase consistent with the fact that resonance enhancement is weaker in the red phase as discussed above. The weak line at 1516 cm⁻¹ assigned to a red phase impurity in the blue phase grows in intensity and becomes the predominant C=C backbone stretching mode in the red phase. From Figure 3b it is evident that the spectrum remains essentially unchanged on cooling consistent with the irreversibility of the red phase of poly-TCDA.

The heating and cooling Raman spectra of poly-TCDA/ZnO with the ZnO content at 5 wt % are shown in Figure 4. By contrast with the variable temperature spectra for pure poly-TCDA, in Figure 4a, a broad scattering band centered near 690 cm⁻¹ appears reproducibly in the spectra with increasing intensity as the temperature approaches and goes above the ca. 120 °C melting transition of the ZnO composites observed in the DSC data (see discussion below and Figure 7). Note that the broad scattering feature appears below the melting transition temperature and increases in intensity above 120

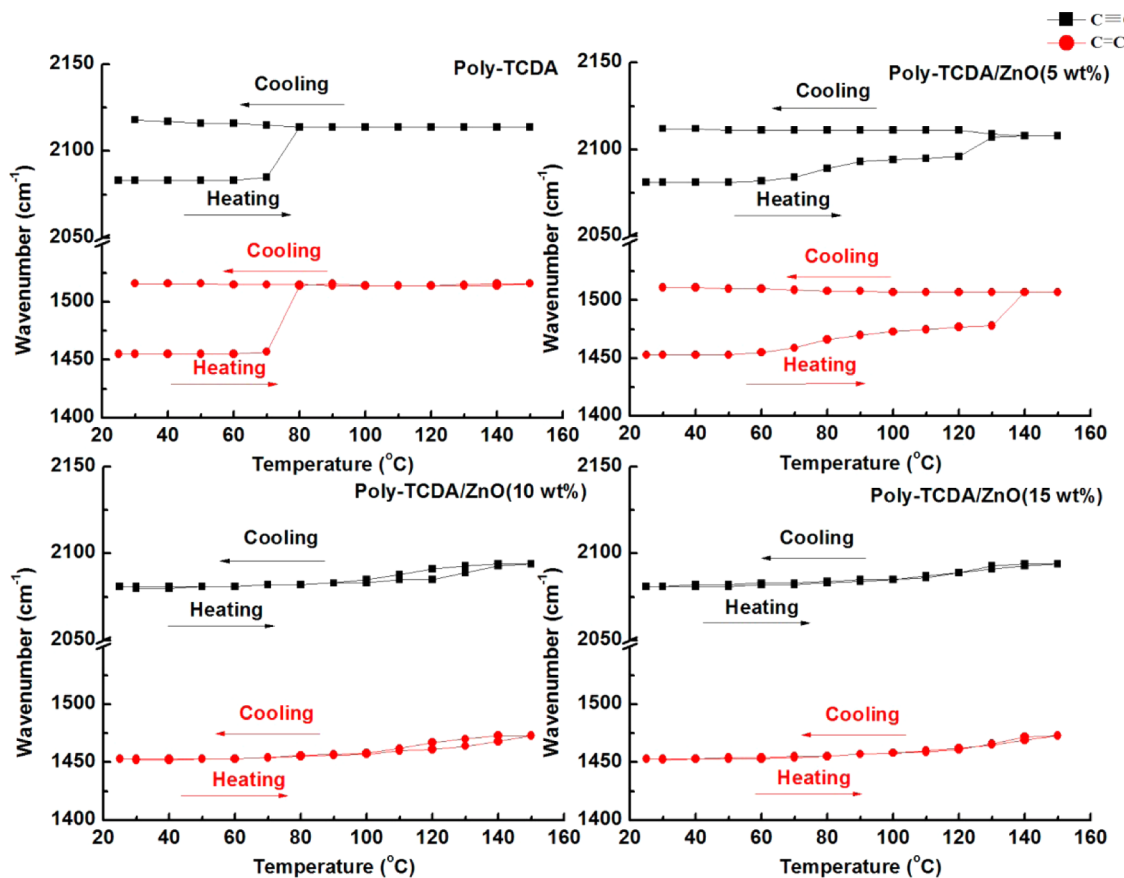


Figure 6. Temperature dependence on heating and cooling of the polymer backbone C≡C and C=C stretching mode frequencies of poly-TCDA and poly-TCDA/ZnO composites with different ZnO contents.

°C. It can be tentatively assigned to light scattering from an amorphous network of the poly-TCDA/ZnO complex. The scattering is not seen at higher ZnO concentrations as discussed below, and it is also not observed in poly-PCDA/ZnO²⁵ at all concentrations of ZnO probably because the diffusional motions of the longer hydrocarbon side chain in poly-PCDA compared with poly-TCDA prevents the formation of the amorphous network. The intensity from the amorphous network shows a small decrease on cooling through the melting temperature down to room temperature in Figure 4b. Moreover, the features of the spectra in Figure 4b show that the red phase of the composite with 5% by weight of ZnO converts only partially back to the blue phase on cooling.

Figure 5 shows the heating and cooling Raman spectra of poly-TCDA/ZnO (15 wt %). Similar heating and cooling Raman spectra (not shown here) were observed for poly-TCDA/ZnO (10 wt %). Broad scattering due to amorphous poly-TCDA/ZnO at these higher ZnO concentrations is not observed (Figure 5a and b). Also, the red phase spectrum changes rapidly back to that of the blue phase on cooling. The Raman frequencies of the C≡C and C=C backbone stretching vibrations of pure poly-TCDA and poly-TCDA with 5, 10, and 15 wt % of ZnO below 100 nm in size as a function of heating and cooling cycles are plotted as a function of temperature in Figure 6. Note that the frequency upshift in the red phase decreases with increasing ZnO content suggesting that the stress on the polymer backbone is lowered due to chelation of ZnO with the head group of poly-TCDA to make the chromatic transition reversible. The plots in Figure 6

of the Raman-active C≡C and C=C backbone stretching frequencies as a function of temperature cycling indicate increases in frequencies at the chromatic blue to red transition at 70 °C on heating for pure poly-TCDA and near 120 °C for the poly-TCDA/ZnO composites. For poly-TCDA/ZnO (5 wt %), the slight upshift of frequency of the C=C and C≡C modes at 70 °C could be due to nonchelated TCDA monomer. The frequency upshift at 130 °C in the composites is due to chelate formation between TCDA and ZnO.

Differential scanning calorimetry (DSC) measurements provide further understanding of the nature of TCDA/poly-TCDA/ZnO interactions. DSC data were obtained for pure TCDA monomer, poly-TCDA, and poly-TCDA/ZnO, at heating and cooling rates of 10 °C min⁻¹ between 25 and 300 °C. The heating scan for pure TCDA in Figure 7a shows an endothermic peak at 61 °C due to melting. On cooling (scan not shown) down-shifted exothermic crystallization peaks at 59 °C due to hysteresis are observed. The heating scan for poly-TCDA in Figure 7b shows an endothermic peak at 61 °C due to melting of the unpolymerized monomer. A broad endotherm with a shoulder at 154 °C and a peak at 190 °C are assigned to the melting of poly-TCDA. On cooling (scan not shown), polymer crystallization is indicated by broad exothermic features at 159 and 194 °C which are upshifted due to hysteresis relative to the corresponding endothermic melting peaks. Crystallization of unpolymerized monomer is not observed during the cooling cycle probably due to loss of the monomer by sublimation during thermal cycling. The heating scans for TCDA–ZnO nanocomposites in Figure 7d

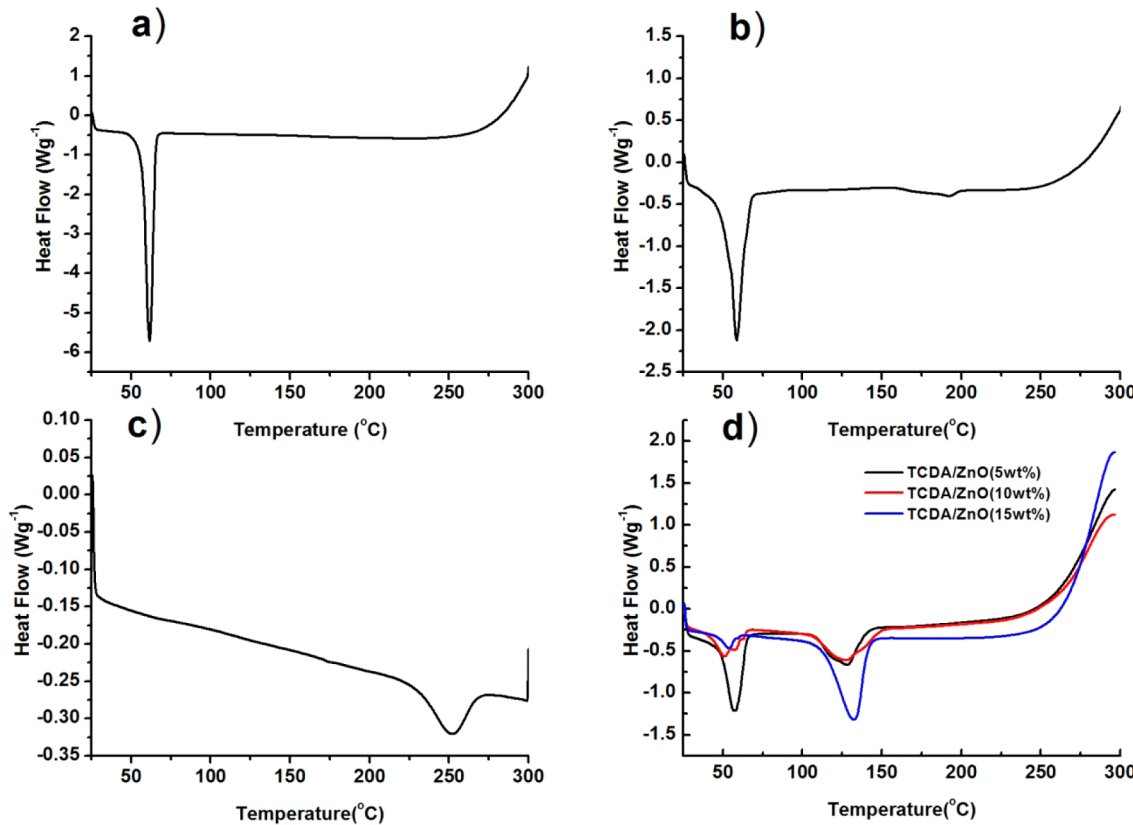


Figure 7. Heating DSC scans for (a) TCDA monomer; (b) poly-TCDA; (c) ZnO nanopowder (<100 nm); (d) TCDA monomer/ZnO nanocomposites of three different compositions. The slightly broadened transition in (b) is due to unpolymerized monomer.

show endotherm around $57\text{ }^{\circ}\text{C}$ due to unpolymerized monomer and a new endothermic feature at around $137\text{ }^{\circ}\text{C}$ due to melting of the monomer modified by chelate formation with ZnO discussed above, which coincides that fact that no endothermic feature of ZnO (Figure 7c) is observed in the DCS data of composites. It is also seen from Figure 7d that with the increase of ZnO content, the endotherm due to TCDA becomes weaker and the peak shifts to higher temperature indicating that the chelate between ZnO and head group $-\text{COOH}$ becomes stronger because more chelate formation can occur with increasing ZnO content. This is consistent with the FTIR, Raman, and DSC data discussed above suggesting an interaction of ZnO particles with the head group of the polymer side chain to form a chelate which can be schematically written as $\text{Zn}^{2+}(\text{COO}^-)_2$. In pure poly-TCDA, heating causes an irreversible stress on the polymer backbone due to the dissociation of hydrogen bonds between the side chain head groups to form the red phase. In the presence of ZnO, chelate formation results in release of strain on cooling and reversal back to the blue phase.

Chroma describes the vividness or dullness of a color, in other words, how close the color is to either gray or the pure hue (Figure 8a). The changes in chromaticity for different samples shown in Figure 8b as a function of temperature further verified the interaction between poly-TCDA and ZnO with increase of ZnO content from 5 to 15 wt %. The rapid increase followed by a drop of the chromaticity of poly-TCDA is caused by the chromatic transition near $70\text{ }^{\circ}\text{C}$. ZnO (5 wt %) increases the chromatic transition to $120\text{ }^{\circ}\text{C}$ consistent with the Raman data. The poly-TCDA/ZnO composites with 10 and 15 wt % have almost the same correlation of chromaticity

and temperature which indicates that there is a critical ZnO content to form the chelate between TCDA and ZnO. Figure 8c and d shows fairly good reversibility in chromaticity as a function of number of cycles from 25 to $80\text{ }^{\circ}\text{C}$ and from 25 to $150\text{ }^{\circ}\text{C}$ indicating that the nanocomposite can function as a very reproducible thermal sensor.

4. CONCLUSIONS

Raman, FTIR, DSC and colorimetric measurements have been used to understand the thermochromic reversibility introduced by composite formation of poly-TCDA with ZnO in the particle size range below 100 nm. Raman frequency upshifts occur at 70 and $120\text{ }^{\circ}\text{C}$ in pure poly-TCDA and poly-TCDA/ZnO composites, respectively, corresponding to chromatic transitions. The peak shifts of the Raman-active $\nu(\text{C}\equiv\text{C})$ and $\nu(\text{C}=\text{C})$ vibration peaks increase with increase of ZnO content. Poly-TCDA/5 wt % ZnO shows only partially reversible color change, whereas poly-TCDA/10 wt % ZnO and poly-TCDA/15 wt % ZnO change color reversibly and have similar thermochromic responses. The Raman data indicate the irreversible formation of an amorphous poly-TCDA phase in poly-TCDA/5 wt % ZnO but not in poly-TCDA composites with 10 and 15 wt % ZnO. Chelate formation between ZnO and neighboring side chain $-\text{COOH}$ head groups is proposed, which leads to reversibility of the chromatic transition and increase of the chromatic transition temperature. Compared with the results of previous study on PCDA, the amorphous feature can be found in poly-TCDA with low concentration of ZnO exclusively, which probably results from the fact that the carbon chain in TCDA is shorter than that in PCDA. Excellent reversibility in chromaticity as a

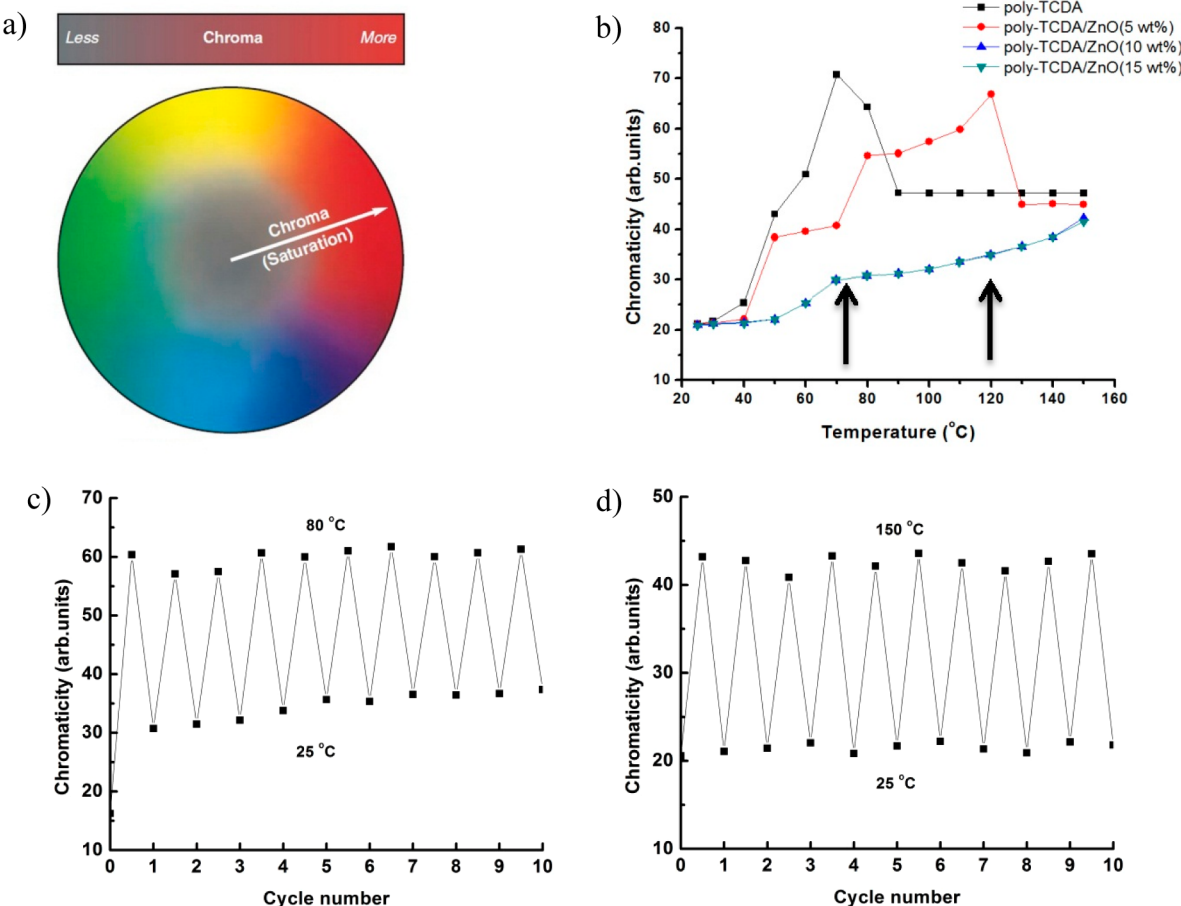


Figure 8. (a) Schematic showing chromaticity (chroma) distribution from gray (dull) color at the center to saturated (vivid) color at the perimeter (arrows indicate chromatic transition temperatures discussed in the text); (b) chromaticity versus temperature plots for poly-TCDA and poly-TCDA/ZnO composites of three different compositions; (c) chromaticity of poly-TCDA/ZnO (5 wt %) as a function of thermal cycle; (d) chromaticity of poly-TCDA/ZnO (15 wt %) as a function of thermal cycle.

function of number of cycles from 25 to 80 °C and from 25 to 150 °C is observed indicating that the poly-TCDA/ZnO nanocomposites can function as a temperature sensor.

AUTHOR INFORMATION

Corresponding Author

* E-mail zafar.iqbal@njit.edu, tel. (973)-596-8571.

Author Contributions

The manuscript was written through contributions of all authors. All authors have given approval to the final version of the manuscript. C.B., Y.Y., and Z.I. contributed equally.

Notes

The authors declare no competing financial interest.

ACKNOWLEDGMENTS

The authors acknowledge support by the U.S. Army contract W15QKN-10-D-0503-0002.

REFERENCES

- (1) Champaiboon, T.; Tumcharern, G.; Potisatityuenyong, A.; Wacharasindhu, S.; Sukwattanasinitt, M. A Polydiacetylene Multilayer Film for Naked Eye Detection of Aromatic Compounds. *Sens. Actuators, B* **2009**, *139*, 532–537.
- (2) Descalzo, A. B.; Dolores Marcos, M.; Monte, C.; Martinez-Manez, R.; Rurack, K. Mesoporous Silica Materials with Covalently Anchored Phenoxazinone Dyes as Fluorescent Hybrid Materials for Vapour Sensing. *J. Mater. Chem.* **2007**, *17*, 4716–4723.
- (3) Janzen, M. C.; Ponder, J. B.; Bailey, D. P.; Ingison, C. K.; Suslick, K. S. Colorimetric Sensor Arrays for Volatile Organic Compounds. *Anal. Chem.* **2006**, *78*, 3591–3600.
- (4) Lu, Y.; Yang, Y.; Sellinger, A.; Lu, M.; Huang, J.; Fan, H.; Haddad, R.; Lopez, G.; Burns, A. R.; Sasaki, D. Y.; et al. Self-Assembly of Mesoscopically Ordered Chromatic Polydiacetylene/Silica Nanocomposites. *Nature* **2001**, *410*, 913–917.
- (5) Muro, M. L.; Daws, C. A.; Castellano, F. N. Microarray Pattern Recognition Based on PtII Terpyridyl Chloride Complexes: Vapochromic and Vapoluminescent Response. *Chem. Commun.* **2008**, 6134–6136.
- (6) Rakow, N. A.; Suslick, K. S. A Colorimetric Sensor Array for Odour Visualization. *Nature* **2000**, *406*, 710–713.
- (7) Robert, W. C.; Darryl, Y. S.; Matthew, S. M.; Eriksson, M. A.; Alan, R. B. Polydiacetylene Films: A Review of Recent Investigations into Chromogenic Transitions and Nanomechanical Properties. *J. Phys.: Condens. Matter* **2004**, *16*, R679–R697.
- (8) Yuan, W.; Jiang, G.; Song, Y.; Jiang, L. Micropatterning of Polydiacetylene Based on a Photoinduced Chromatic Transition and Mechanism Study. *J. Appl. Polym. Sci.* **2007**, *103*, 942–946.
- (9) Hammond, P. T.; Rubner, M. F. Thermochromism in Liquid Crystalline Polydiacetylenes. *Macromolecules* **1997**, *30*, 5773–5782.
- (10) Huang, X.; Jiang, S.; Liu, M. Metal Ion Modulated Organization and Function of the Langmuir–Blodgett Films of Amphiphilic Diacetylene: Photopolymerization, Thermochromism, and Supramolecular Chirality. *J. Phys. Chem. B* **2004**, *109*, 114–119.

- (11) Peng, H.; Tang, J.; Pang, J.; Chen, D.; Yang, L.; Ashbaugh, H. S.; Brinker, C. J.; Yang, Z.; Lu, Y. Polydiacetylene/Silica Nanocomposites with Tunable Mesostructure and Thermochromatism from Diacetylenic Assembling Molecules. *J. Am. Chem. Soc.* **2005**, *127*, 12782–12783.
- (12) Peng, H.; Tang, J.; Yang, L.; Pang, J.; Ashbaugh, H. S.; Brinker, C. J.; Yang, Z.; Lu, Y. Responsive Periodic Mesoporous Polydiacetylene/Silica Nanocomposites. *J. Am. Chem. Soc.* **2006**, *128*, 5304–5305.
- (13) Ahn, D. J.; Chae, E. H.; Lee, G. S.; Shim, H. Y.; Chang, T. E.; Ahn, K. D.; Kim, J. M. Colorimetric Reversibility of Polydiacetylene Supramolecules Having Enhanced Hydrogen-Bonding under Thermal and pH Stimuli. *J. Am. Chem. Soc.* **2003**, *125*, 8976–8977.
- (14) Kim, J.; Lee, J.; Choi, H.; Sohn, D.; Ahn, D. J. Rational Design and in-Situ FTIR Analyses of Colorimetrically Reversible Polydiacetylene Supramolecules. *Macromolecules* **2005**, *38*, 9366–9376.
- (15) Lee, S.; Kim, J. M. Alpha-Cyclodextrin: A Molecule for Testing Colorimetric Reversibility of Polydiacetylene Supramolecules. *Macromolecules* **2007**, *40*, 9201–9204.
- (16) Park, H.; Lee, J. S.; Choi, H.; Ahn, D. J.; Kim, J. M. Rational Design of Supramolecular Conjugated Polymers Displaying Unusual Colorimetric Stability upon Thermal Stress. *Adv. Funct. Mater.* **2007**, *17*, 3447–3455.
- (17) Yuan, Z.; Lee, C. W.; Lee, S. H. Reversible Thermochromism in Hydrogen-Bonded Polymers Containing Polydiacetylenes. *Angew. Chem.* **2004**, *116*, 4293–4296.
- (18) Gu, Y.; Cao, W.; Zhu, L.; Chen, D.; Jiang, M. Polymer Mortar Assisted Self-Assembly of Nanocrystalline Polydiacetylene Bricks Showing Reversible Thermochromism. *Macromolecules* **2008**, *41*, 2299–2303.
- (19) Song, J.; Cisar, J. S.; Bertozzi, C. R. Functional Self-Assembling Bolaamphiphilic Polydiacetylenes as Colorimetric Sensor Scaffolds. *J. Am. Chem. Soc.* **2004**, *126*, 8459–8465.
- (20) Li, L. S.; Stupp, S. I. Two-Dimensional Supramolecular Assemblies of a Polydiacetylene. 2. Morphology, Structure, and Chromic Transitions. *Macromolecules* **1997**, *30*, 5313–5320.
- (21) Yang, Y.; Lu, Y.; Lu, M.; Huang, J.; Haddad, R.; Xomeritakis, G.; Liu, N.; Malanoski, A. P.; Sturmayr, D.; Fan, H.; et al. Functional Nanocomposites Prepared by Self-Assembly and Polymerization of Diacetylene Surfactants and Silicic Acid. *J. Am. Chem. Soc.* **2003**, *125*, 1269–1277.
- (22) Baughman, R. H. Solid-State Polymerization of Diacetylenes. *J. Appl. Phys.* **1972**, *43*, 4362–4370.
- (23) Lim, K. C.; Heeger, A. J. Spectroscopic and Light Scattering Studies of the Conformational (Rod-to-Coil) Transition of Poly(diacetylene) in Solution. *J. Chem. Phys.* **1985**, *82*, 522–530.
- (24) Chance, R. R.; Baughman, R. H.; Muller, H.; Eckhardt, C. J. Thermochromism in a Polydiacetylene Crystal. *J. Chem. Phys.* **1977**, *67*, 3616–3618.
- (25) Patlolla, A.; Zunino, J.; Frenkel, A. I.; Iqbal, Z. Thermochromism in Polydiacetylene–Metal Oxide Nanocomposites. *J. Mater. Chem.* **2012**, *22*, 7028–7035.
- (26) Lim, C.; Sandman, D. J.; Sukwattanasinitt, M. Topological Polymerization of *tert*-Butylcalix[4]arenes Containing Diynes. *Macromolecules* **2007**, *41*, 675–681.